

Theoretical Investigation of the (Hyper)polarizabilities of Pyrrole Homologues C₄H₄XH (X = N, P, As, Sb, Bi). A Coupled-Cluster and Density Functional Theory Study

Andrea Alparone[†]

Dipartimento di Scienze Chimiche, Università di Catania, Viale A. Doria 8, 95125 Catania, Italy

Heribert Reis[†] and Manthos G. Papadopoulos[†]

Institute of Organic and Pharmaceutical Chemistry, National Hellenic Research Foundation, 48 Vassileos Constantinou, Athens 11635, Greece

Received: December 22, 2005; In Final Form: February 28, 2006

Geometries, inversion barriers, static and dynamic electronic and vibrational dipole polarizability (α), and first (β) and second (γ) hyperpolarizability of the pyrrole homologues C₄H₄XH (X = N, P, As, Sb, Bi) have been calculated by Hartree–Fock, Møller–Plesset second-order perturbation theory, coupled-cluster theory accounting for singles, doubles, and noniterative triple excitations methods, as well as density functional theory using B3LYP and PBE1PBE functionals and Sadlej's Pol and 6-311G** basis sets. Relativistic effects on the heavier homologues stibole and bismole have been taken into account within effective core potential approximation. The results show that the electronic (hyper)polarizabilities monotonically increase with the atomic number of the heteroatom, consistent with the decrease in the molecular hardness. Ring planarization reduces the carbon–carbon bond length alternation of the *cis*-butadienic unit, enhancing the electronic polarizability values ($\langle\alpha^e\rangle$) by 4–12% and the (hyper)polarizability values (β_{vec}^e and $\langle\gamma^e\rangle$) by 30–90%. Pure vibrational and zero-point vibrational average contributions to the (hyper)polarizabilities have been determined within the clamped nucleus approach. In the static limit, the pure vibrational hyperpolarizabilities have a major contribution. Anharmonic corrections dominate the pure vibrational hyperpolarizabilities of pyrrole, while they are less important for the heavier homologues. Static and dynamic electronic response properties of the pyrrole homologues are comparable to or larger than the corresponding properties of the furan and cyclopentadiene homologue series.

1. Introduction

Organic π -conjugated oligomers and polymers have attracted considerable interest in the search for new materials suitable for optoelectronic and photonic devices.¹ Five-membered heterocycles such as thiophene (C₄H₄S) and pyrrole (C₄H₄NH) are promising candidates as the building blocks of organic conductors as well as of oligomers and polymers for nonlinear optical (NLO) applications.^{2,3} Polypyrrole is stable in air⁴ and, upon doping, exhibits large second-order NLO responses and high electrical conductivities.³ Experimentally, the dipole polarizability, α , of pyrrole has been measured in carbon tetrachloride⁵ and dioxane⁶ solutions, whereas both the first, β , and second, γ , hyperpolarizabilities are yet unknown. From computational work, some estimates of the α , β , and γ of pyrrole have been previously reported.^{7–12}

Very little is known of the effect of heteroatom substitution on the (hyper)polarizabilities of the pyrrole homologues. Hinchliffe and Soscun Machado¹⁰ reported ab initio computations of the static electronic dipole polarizability, $\alpha^e(0;0)$, and first hyperpolarizability, $\beta^e(0;0,0)$, of pyrrole and phosphole (C₄H₄PH). Albert et al.¹³ investigated dynamic β^e values of some 2- and 2,5-substituted pyrrole and phosphole derivatives at the semiempirical INDO/1 level. More recently, Delaere et al.¹¹ computed $\alpha^e(0;0)$ values of a series of oligomers of pyrrole and

phosphole, including the monomer, by using density functional theory (DFT). Both $\alpha^e(0;0)$ ^{10,11} and $\beta^e(0;0)$ values of phosphole are larger than those of pyrrole and thiophene, consistent with its smaller highest occupied molecular orbital to lowest unoccupied molecular orbital (HOMO–LUMO) energy gap.^{10,11} Compared to its nitrogen counterpart, the chemistry of phosphole is much less known (for reviews on phospholes, see ref 14). Recent studies have established that π -organophosphorus molecules incorporating the phosphole unit are promising materials for organic light-emitting diodes.¹⁵ The experimental molecular structure of phosphole is not available, although X-ray structures of some phosphole derivatives have been reported.^{16,17} Contrary to pyrrole, phosphole derivatives exhibit a nonplanar structure,^{16,17} the aromatic stabilization of the planar form being insufficient to overcome the barrier to the pyramidal inversion at the phosphorus atom, which was estimated to be ~ 16 kcal/mol from NMR spectroscopic investigations.¹⁷ However, recent works on phosphole derivatives have shown that the insertion of either bulky substituents at phosphorus or the π -electron acceptor group at position 2 favors a major overlap of the lone-pair orbital with the π *cis*-butadienic moiety, increasing the planarity and aromatic stabilization in the ring.¹⁸ Similarly, the ground-state structure of the heavier homologues, arsole (C₄H₄AsH), stibole (C₄H₄SbH), and bismole (C₄H₄BiH) are predicted to be nonplanar.^{19–21} The energy barrier to inversion at the heteroatom is predicted to increase with the atomic number of the heteroatom.^{20,21} On the other hand, the

[†] E-mail address: agalparone@dipchi.unict.it (A.A.); hreis@eie.gr (H.R.); mpapad@eie.gr (M.G.P.).

HOMO–LUMO energy gap of the pyrrole homologues decreases with the atomic number of the heteroatom,²¹ suggesting an increase in the (hyper)polarizabilities along the series.

In this work, we present ab initio coupled-cluster (CC) and DFT calculations of the dipole polarizability and the first and second dipole hyperpolarizabilities of the pyrrole homologues C₄H₄XH (X = N, P, As, Sb, Bi) to investigate the effects of heteroatom replacement and ring planarization on these properties. Response properties of arsole, stibole, and bismole are computed here for the first time. Frequency-dependent (hyper)polarizabilities and vibrational contributions are also computed. Recent calculations on pyrrole⁸ and on 2,2'-bipyrrole and 2,2':5',2''-terpyrrole²² have shown that vibrational terms are important contributors to the total (hyper)polarizabilities. The results are compared with previously reported results on cyclopentadiene homologues, C₄H₄XH₂ (X = C, Si, Ge, Sn) and furan homologues, C₄H₄X (X = O, S, Se, Te).

2. Computational Methods

The molecular geometries of C₄H₄XH (X = N, P, As, Sb, Bi) were fully optimized under C_s and C_{2v} symmetries at the DFT level using the B3LYP functional with the Pol basis sets.^{23–25} The dipole moments (μ), static- and frequency-dependent electronic dipole polarizability (α^e), and first (β^e) and second (γ^e) dipole hyperpolarizabilities were calculated analytically within time-dependent Hartree–Fock theory (TDHF)²⁶ using the Pol basis sets. Electron correlation effects were introduced by ab initio Møller–Plesset second-order perturbation theory (MP2), CC theory accounting for singles and doubles (CCSD) and noniterative triple excitations (CCSD(T)), and by DFT methods employing the B3LYP and the most recent PBE1PBE functional.²⁷ Correlated calculations were carried out with the finite-field (FF) method as described in ref 28. The selection of the electric field strength (F) is crucial for the accuracy of FF results.^{28,29} An adequate F value must be small enough to avoid contamination from higher order hyperpolarizability contributions but sufficiently high to attain the required numerical accuracy. In the case of pyrrole, we performed FF–HF calculations at different field strengths in the 10^{−3}–10^{−2} au range. The (hyper)polarizability values thus obtained were compared with the analytically computed data. The best agreement was obtained for an F value of 0.005 au, for which numerical and analytic α^e , β^e , and γ^e values agree within 0.02, 2.1, and 2.2%, respectively.

Estimated CCSD(T) dynamic response properties, $P^e(\omega)^{\text{CCSD(T)}}$, were obtained through a multiplicative scaling method by using HF dispersion ratios, as commonly adopted in the literature:³⁰

$$P^e(\omega)^{\text{CCSD(T)}} = \frac{P^e(\omega)^{\text{HF}}}{P^e(0)^{\text{HF}}} P^e(0)^{\text{CCSD(T)}} \quad (1)$$

It is known from previous investigations that relativistic corrections are necessary for an accurate determination of the (hyper)polarizabilities of systems containing heavy atoms.^{31–33} Relativistic effects on the electronic properties of the heaviest homologues, stibole and bismole, were taken into account within the quasirelativistic effective core potential (ECP) method, used together with the corresponding valence electron basis sets developed by the Stuttgart group,³⁴ and further augmented with the most polarized and diffused Pol functions (ECP–Pol), similarly to the method recently employed for the (hyper)polarizability calculations by Norman et al.³² for XH (X = F,

Cl, Br, I, At) and XH₂ (X = O, S, Se, Te, Po) and by Jansik et al.³³ for C₄H₄X (X = O, S, Se, Te) systems.

Vibrational contributions of C₄H₄XH (X = N, P, As, Sb) were computed in the usual clamped nucleus approximation.³⁵ The vibrational properties were separated into pure vibrational (PV) and zero-point vibrational average (ZPVA) contributions. PV contributions can be quite large in the static field limit, but are often strongly quenched at optical frequencies. The frequency dispersion of ZPVA contributions resembles more closely the one of the electronic contribution. Vibrational contributions were calculated according to Bishop–Kirtman perturbation theory (BKPT),^{35,36} where the perturbation terms are sorted according to the level of mechanical and electric anharmonicities. For these computations, second and higher-order derivatives of the energy as well as first and higher-order derivatives of electric properties with respect to normal coordinates are required. In the symbolic (n, m) notation of Bishop and Kirtman, where m and n denote the level of mechanical and electrical anharmonicity, respectively, the first-order ZPVA contribution P^{ZPVA} to an electrical property P is

$$P^{\text{ZPVA}} = [P]^{1,0} + [P]^{0,1} = -\frac{\hbar}{4} \sum_a \left[\sum_b \frac{F_{\text{abb}}}{\omega_b \omega_a^2} \frac{\partial P^{\text{el}}}{\partial Q_a} - \frac{1}{\omega_a} \frac{\partial^2 P^{\text{el}}}{\partial Q_a^2} \right] \quad (2)$$

where Q_a and ω_a are normal coordinates and vibrational frequencies, respectively, and F_{abb} is a cubic anharmonic force constant (third-order derivative of the energy with respect to normal coordinates). P may be any component of μ , α , β , or γ , and P^{el} denotes the electronic contribution to P . In the same (n, m) notation, the PV contributions up to the second order in total ($n + m = 2$) are

$$\alpha^{\text{PV}} = [\mu^2]^{0,0} + [\mu^2]^{\text{II}} \quad (3)$$

$$\beta^{\text{PV}} = [\mu\alpha]^{0,0} + [\mu^3]^{0,1} + [\mu\alpha]^{\text{II}} \quad (4)$$

$$\gamma^{\text{PV}} = [\alpha^2]^{0,0} + [\mu\beta]^{0,0} + [\mu^2\alpha]^{0,1} + [\mu^4]^{0,2} + [\mu^2\alpha]^{\text{II}} + [\mu\beta]^{\text{II}} \quad (5)$$

where $[\]^0 = [\]^{0,0}$, $[\]^1 = [\]^{1,0} + [\]^{0,1}$, $[\]^{\text{II}} = [\]^{2,0} + [\]^{1,1} + [\]^{0,2}$, and the bracketed terms are functions of derivatives of the Hessian and electric properties with respect to the normal coordinates (see ref 36 for explicit expressions). At the so-called double-harmonic approximation, only the $[\]^0$ contributions are retained.

The crux of the computation of the vibrational contributions is the calculation of the higher-order derivatives. At the SCF level and with a modest number of basis functions, CADPAC, version 5³⁷ allows the analytical computation of property derivatives of order $mnpq = 43210$, where m, n, o, p , and q refer to the order of derivative of the energy, dipole moment, polarizability, and the first and second hyperpolarizabilities, respectively. With these derivatives, all terms of α^{PV} in eq 3, all $[\]^0$ and $[\]^1$ terms, as well as many of the $[\]^{\text{II}}$ terms of β^{PV} and γ^{PV} can be computed. However, the ZPVA contributions to the hyperpolarizabilities are not accessible.

A more generally applicable method computes numerical derivatives either employing geometrical displacements³⁸ or finite electric fields.³⁹ By a combination of these numerical methods, derivatives up to order $mnpq = 32222$ can be computed, even for comparatively large molecules with modest computational effort,³⁹ which allows the computation of ZPVA

contributions to all electrical properties up to the second hyperpolarizability.

We have used analytical methods to compute static PV contributions for C_4H_4XH ($X = N, P, As$) at the SCF level up to the highest order of derivatives achievable ($mnopq = 43210$), which allowed us to investigate the important question of the *initial convergence* of the perturbation series,⁴⁰ employing the 6-311G** basis set. Numerical derivative methods were used to compute property derivatives up to $mnopq = 32222$ for the same molecules with the 6-311G** basis set and for C_4H_4SbH with the Pol basis set, as there is no 6-311G** basis for Sb available. To investigate electron correlation effects, PV contributions for α and β at the MP2 level were computed for C_4H_4XH ($X = N, P, As$) with the same basis sets as those used for the SCF computations. The computation of vibrational properties for C_4H_4BiH as well as for C_4H_4SbH at the MP2 level proved to be infeasible with the computational resources available.

All derivative computations were performed at the geometry optimized with the same level and basis set combination.

In the tables, we report the isotropically averaged polarizability and the first and second hyperpolarizabilities, which are respectively defined as

$$\langle \alpha \rangle = \frac{1}{3}(\alpha_{xx} + \alpha_{yy} + \alpha_{zz})$$

$$\beta_{vec} = \frac{3}{5} \sqrt{\beta_x^2 + \beta_z^2}$$

where β_i ($i = x, z$) is given by

$$\beta_i = \frac{1}{3} \sum_{j=x,y,z} (\beta_{ijj} + \beta_{jji} + \beta_{jji})$$

and

$$\langle \gamma \rangle = \frac{1}{15} \sum_{ij} (\gamma_{ijij} + \gamma_{ijji} + \gamma_{ijji})$$

where $i, j = x, y, z$. Individual μ_i , α_{ij} , β_{ijk} , and γ_{ijkl} components computed within our choice of coordinate system are available as Supporting Information (Tables S3–S7).

Geometry, dipole moment, as well as static electronic (hyper)polarizability calculations were carried out with Gaussian 03.⁴¹ Frequency-dependent (hyper)polarizabilities were performed with the GAMESS program.⁴² For the computation of vibrational contributions to the (hyper)polarizabilities, the CADPAC 5,³⁷ CADPAC 6,⁴³ and SPECTRO⁴⁴ program packages were also used.

3. Results and Discussion

3.1. Geometries, Barrier to Pyramidal Inversion, and Atomization Energy. The geometries of pyrrole homologues C_4H_4XH ($X = N, P, As, Sb, Bi$) were optimized under C_{2v} and C_s symmetry constraints at the B3LYP/Pol level, and that of bismole was optimized at the B3LYP/ECP–Pol level. B3LYP/Pol harmonic vibrational analysis shows that the neutral equilibrium structure of pyrrole is planar. By contrast, the ground state of C_4H_4XH ($X = P, As, Sb, Bi$) is predicted to have a pyramidal arrangement at the heteroatom, in agreement with experimental X-ray diffraction studies of some phosphole derivatives.^{16,17} The planar C_{2v} structure of C_4H_4XH ($X = P, As, Sb, Bi$) corresponds to the transition state (one imaginary frequency) to the pyramidal inversion at the heteroatom.

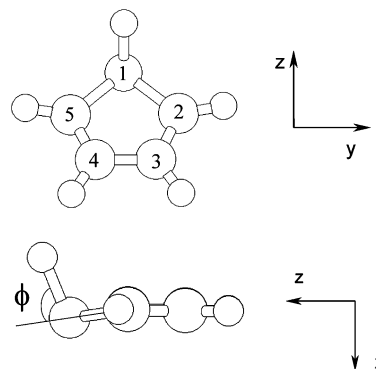


Figure 1. Coordinate system and atomic numbering of the investigated molecules.

The computed geometrical parameters of pyrrole are in reasonable agreement with the gas-phase microwave values,⁴⁵ giving root-mean-square deviations of 0.01 Å and 0.2° for bond lengths and bond angles, respectively, while for phosphole, current calculations overestimate the X-ray P–C, C–C, and C=C bond lengths of 1-benzyl-phosphole¹⁶ by ~0.02 Å, presumably due to solid-state effects. It is important to note that, for bismole, the quasirelativistic corrections included in the ECP–Pol basis set shorten both the X–C and X–H bond lengths with respect to the Pol data by 0.024 and 0.015 Å, respectively. In the C_4H_4XH ($X = P, As, Sb, Bi$) molecules, the angle at the X atom, ϕ (Figure 1), monotonically increases along the series from 74° to 85°, while the sum of the C–X–C and C–X–H angles decreases from 292° to 266°, indicating an increase in the pyramidalization as the heteroatom becomes heavier. As expected, upon proceeding from the pyramidal to the planar structure, the C=C becomes longer and the C–C bond length becomes shorter by 0.020–0.034 Å and 0.029–0.035 Å, respectively. Thus, in passing from the C_s to the C_{2v} form, the CC bond length alternation (Δ_{CC}), defined as the difference between the lengths of single and double bonds, is reduced by 0.05–0.07 Å. These results are consistent with experimental findings, which show that, in passing from the pyramidalized structure of 1-benzyl-phosphole¹⁶ to the more planar 1-(2,4,6-tri-*tert*-butylphenyl)-3-methylphosphole,⁴⁶ the Δ_{CC} value decreases by 0.04 Å. The present results are in substantial agreement with those recently obtained by Pelzer et al.²¹ on the same molecules by MP2 and B3LYP calculations with a basis set of triple- ζ quality.

The different degrees of pyramidalization and thermodynamic stability of the heterocycles reflect on the barrier to inversion at the heteroatom and atomization energy, respectively. Barrier inversions of C_4H_4XH ($X = P, As, Sb, Bi$) were evaluated by comparing the energies of the planar and pyramidal structures, $\Delta E_{inv} = E_{C_{2v}} - E_{C_s}$. The ΔE_{inv} value monotonically increases along the series, consistent with the structural properties. The present CCSD(T)/Pol ΔE_{inv} values are 19.3, 28.6, 35.9, and 55.9 kcal/mol for phosphole, arsole, stibole, and bismole, respectively. The corresponding B3LYP/Pol values are 16.9, 27.7, 35.3, and 52.2 kcal/mol, respectively. Zero-point vibrational energy (ZPVE) corrections, computed at the B3LYP/Pol level, are small, reducing the ΔE_{inv} values by 0.4–0.6 kcal/mol. NMR spectroscopy studies of some substituted phospholes give ΔE_{inv} values close to 16 kcal/mol,¹⁷ in reasonable agreement with the present correlated estimates. The B3LYP/Pol atomization energies (ΣD_0), evaluated as the difference between the sum of the atomic energies and the ground-state molecular energy corrected for the ZPVE, are 43.7, 40.8, 39.8, 38.9, and 38.6 eV for pyrrole, phosphole, arsole, stibole, and

TABLE 1: Dipole Moments (au) and Electronic Dipole (Hyper)polarizabilities (au) of C₄H₄XH (X = N, P, As, Sb, Bi)^a

	μ	$\langle\alpha^e\rangle$	β_{vec}	$\langle\gamma\rangle$
C ₄ H ₄ NH				
HF/Pol	0.730	53.70	27.5	16345
MP2/Pol	0.739	55.24	34.7	20255
CCSD(T)/Pol	0.727	54.87	44.0	18838
PBE1PBE/Pol	0.728	54.68	19.3	19524
PBE1PBE/ECP–Pol	0.734	54.93	18.4	19588
expt	0.685 ^b			
	0.700 ^c	53.56 ^c		
		55.80 ^d		
C ₄ H ₄ PH				
HF/Pol	0.437	70.42	88.4	18022
MP2/Pol	0.328	72.11	76.3	24404
CCSD(T)/Pol	0.340	71.39	74.3	23027
PBE1PBE/Pol	0.334	72.19	83.6	23425
PBE1PBE/ECP–Pol	0.315	72.35	93.7	23642
C ₄ H ₄ AsH				
HF/Pol	0.363	75.21	137.8	19578
MP2/Pol	0.291	76.74	121.6	26595
CCSD(T)/Pol	0.294	76.12	122.3	25696
PBE1PBE/Pol	0.276	77.00	124.2	26336
PBE1PBE/ECP–Pol	0.233	77.12	134.4	26558
C ₄ H ₄ SbH				
HF/Pol	0.258	87.61	294.4	27584
MP2/Pol	0.208	89.34	261.8	36541
CCSD(T)/Pol	0.215	88.74	265.0	35874
PBE1PBE/Pol	0.205	89.59	249.6	36240
PBE1PBE/ECP–Pol	0.127	89.09	274.0	36051
C ₄ H ₄ BiH				
HF/Pol	0.155	94.43	399.3	32650
MP2/ECP–Pol ^e	0.326	94.54	401.1	40418
CCSD(T)/ECP–Pol ^e	0.327	93.99	406.9	39306
PBE1PBE/Pol	0.128	96.30	341.5	42461
PBE1PBE/ECP–Pol ^e	0.268	94.07	379.6	39521

^a Calculations were carried out on the B3LYP/Pol equilibrium geometry. ^b Reference 45. ^c Reference 5. ^d Reference 6. ^e Calculations were carried out on the B3LYP/ECP–Pol equilibrium geometry.

bismole, respectively. As expected, ΣD_0 decreases along the series, consistent with the trend of the energy difference for bond dissociation previously evaluated at the HF/3-21G* level for C₄H₄XH (X = N, P, As, Sb).¹⁹

The geometrical parameters and inversion barriers are available as Supporting Information (Tables S1 and S2, respectively).

3.2. Atomic Charges and Dipole Moments. Atomic charges of the studied molecules were evaluated within the generalized atomic polar tensor (GAPT) method.⁴⁷ For pyrrole, the B3LYP/Pol GAPT charge on the nitrogen is -0.335 e, while, for the heavier homologues, the GAPT_X charge is positive, being 0.226, 0.361, 0.527, and 0.602 e for phosphole, arsole, stibole, and bismole, respectively. These results are consistent with the “spectroscopic electronegativity” of the X atom (χ_X) estimated by Allen,⁴⁸ which decreases as the atomic number increases ($\chi_N = 3.066$, $\chi_P = 2.253$, $\chi_{As} = 2.211$, $\chi_{Sb} = 1.984$), and a linear relationship is established between the χ_X and GAPT_X charge values ($r^2 = 0.99$). A similar correlation was recently found in the cyclopentadiene homologue series.⁴⁹

Dipole moments of the studied molecules are collected in Table 1. The experimental dipole moment of pyrrole is known to be 0.685 au in the gas phase⁴⁵ and 0.700 au in CCl₄ solution,⁵ whereas the experimental μ data of the heavier homologues are unavailable. The CCSD(T)/Pol μ value of pyrrole is 0.727 au, in reasonable agreement with the experimental data. The present μ values computed with the Pol basis sets monotonically decrease along the series. The ECP–Pol basis sets, which

contain approximate relativistic contributions, modify the μ order in the series. In the present case, the most significant variations are obtained for the heaviest molecule, bismole, so that, in passing from the Pol to the ECP–Pol basis set, the μ value is more than doubled, consistent with an increase in the GAPT charge on the BiH group by 0.1 e. Note that, in the related bismuth hydride molecule (BiH₃), the introduction of quasirelativistic corrections gives a similar increase in μ .²⁵ Accordingly, the order of the ECP–Pol results becomes

$$\mu(\text{pyrrole}) > \mu(\text{phosphole}) > \mu(\text{bismole}) > \mu(\text{arsole}) > \mu(\text{stibole})$$

3.3. Electronic Dipole Polarizabilities. Static electronic dipole polarizabilities of the investigated molecules are reported in Table 1. Experimentally, polarizability values of pyrrole are available from depolarization ratios, refraction, and dielectric polarization measurements in carbon tetrachloride solution at $\lambda = 589.3$ nm,⁵ and from Kerr effect measurements in dioxane solution at $\lambda = 633$ nm,⁶ whereas the α values of the heavier homologues are unknown. At the CCSD(T) level of theory, static (α^e) values of pyrrole, phosphole, arsole, stibole, and bismole are 54.87, 71.39, 76.12, 88.74, and 93.99 au, respectively. Inclusion of electron correlation gives small and positive corrections to the polarizabilities, thus the CCSD(T) theory increases the HF $\langle\alpha^e\rangle$ values by 1–2%. A comparison of $\langle\alpha^e\rangle$ values obtained at all the correlated levels employed shows that the differences between them are small. We note that the present correlated $\langle\alpha^e\rangle$ values of pyrrole compare very well with the previous best estimates of El-Bakali Kassimi et al.⁷ at the MP2/[5s3p2d/3s2p] level (54.91 au) and Jug et al.⁸ at the LDA/TZVP+FIP/LDA/DZVP level (55.77 au). Contrary to the dipole moment, $\langle\alpha^e\rangle$ values do not vary substantially with the basis sets, implying that relativistic effects are negligible. These results are consistent with recent calculations on HX (X = F, Cl, Br, I, At), H₂X (X = O, S, Se, Te, Po),³² and C₄H₄X (X = O, S, Se, Te) systems,³³ where HF/Pol and HF/ECP–Pol α_{ii}^e values are very close to each other.

To make a more appropriate comparison with the experimental data, frequency-dependent electronic polarizabilities were evaluated at the HF/Pol/B3LYP/Pol level. The frequency dependence of $\langle\alpha^e\rangle$ can be represented by an even-order power-series expansion of ω :⁵⁰

$$\langle\alpha^e\rangle(\omega;\omega) = \langle\alpha^e\rangle(0;0)[1 + A'\omega^2 + B'\omega^4 + \dots] \quad (6)$$

where A, B, ... are the second-, fourth-, ... order expansion coefficients, which may be useful to directly compare experimental and theoretical dynamic values.⁵¹ A' and B' coefficients, determined from a least-squares fitting procedure of eq 6 truncated to the fourth-order of ω using $\langle\alpha^e\rangle(\omega;\omega)$ values in the $\hbar\omega = 0-0.072$ au range are listed in Table 2. Both A' and B' values increase upon going from pyrrole to bismole. It was observed that the $1/\sqrt{A'}$ value gives an upper bound to the first dipole-allowed electronic excitation energy.⁵² Values of $1/\sqrt{A'}$ are 0.409, 0.383, 0.384, 0.354, and 0.341 au for pyrrole, phosphole, arsole, stibole and bismole, respectively. It is worth noting that these values are smaller than the corresponding ones in the series of furan homologues, C₄H₄X (X = O, S, Se, Te),⁵³ and cyclopentadiene homologues, C₄H₄XH₂ (X = C, Si, Ge, Sn),⁵⁴ which are in the 0.361–0.417 and 0.390–0.425 au ranges, respectively.

For the molecules studied at the experimental He/Ne laser wavelength $\lambda = 632.8$ nm ($\hbar\omega = 0.072$ au), the dispersion corrections to $\langle\alpha^e\rangle$ amount to 3–4% of the static value, to be

TABLE 2: Coefficients A^i (au) and B^i (au) of the Power-Series Expansions of the Dynamic Electronic (Hyper)polarizabilities of C_4H_4XH (X = N, P, As, Sb, Bi)^a

	C_4H_4NH		C_4H_4PH		C_4H_4AsH		C_4H_4SbH		C_4H_4BiH	
	A^i	B^i	A^i	B^i	A^i	B^i	A^i	B^i	A^i	B^i
$\langle\alpha^e\rangle(-\omega;\omega)^b$	5.98	77.10	6.81	102.54	6.77	94.14	7.98	123.79	8.60	139.53
$\beta_{vec}^e(-2\omega;\omega,\omega)^c$	7.00	-49.19	11.65	101.63	12.21	129.03	14.79	203.42	15.80	241.57
$\beta_{vec}^e(-\omega;\omega,0)^c$	6.95	-31.39	11.67	96.41	12.26	118.13	14.89	180.43	15.94	211.28
$\langle\gamma^e\rangle(-3\omega;\omega,\omega,\omega)^d$	18.18	395.28	15.83	271.56	15.76	262.21	18.17	372.26	19.36	436.96
$\langle\gamma^e\rangle(-2\omega;\omega,\omega,0)^d$	18.59	339.90	16.07	239.69	15.99	231.48	18.54	319.02	19.83	368.60
$\langle\gamma^e\rangle(-\omega;\omega,\omega,-\omega)^d$	18.65	346.21	16.10	239.47	16.02	232.43	18.59	314.03	19.90	359.94
$\langle\gamma^e\rangle(-\omega;\omega,0,0)^d$	18.70	303.80	16.13	217.63	16.04	211.95	18.63	288.23	19.94	330.31

^a Calculations were carried out at the HF/Pol level on the B3LYP/Pol equilibrium geometry. ^b See eq 6. ^c See eq 7. ^d See eq 8.

compared with a value of 3.5% formerly obtained on pyrrole at $\lambda = 602$ nm by TDHF/4-31G+pd calculations.⁹ For pyrrole at $\hbar\omega = 0.072$ au, the introduction of the CCSD(T) corrections to the dynamic HF/Pol α_{ii}^e values, through eq 1, gives an $\langle\alpha^e\rangle(\omega;\omega)$ value of 56.68 au, in good agreement with the experimental datum of 55.80 au by Calderbank et al.⁶

At all levels of theory, the polarizability components increase monotonically along the series, with the major variations being found in passing from pyrrole to phosphole, where $\langle\alpha^e\rangle$ increases by $\sim 30\%$. Interestingly, the polarizability of the heterocycles are found to be in excellent linear correlation with the polarizability of the corresponding X atoms (at the HF/POL level, the $\langle\alpha^e\rangle(0;0)$ values are 7.26, 25.15, 30.29, 45.01, and 52.88 au for N, P, As, Sb, and Bi, respectively) ($r^2 = 1.00$) as well as hydrides, XH_3 (at the HF/POL level, the $\langle\alpha^e\rangle(0;0)$ values are 13.34, 30.30, 35.34, 47.40, and 54.07 au for NH_3 , PH_3 , AsH_3 , SbH_3 , and BiH_3 , respectively) ($r^2 = 1.00$), with 0.9 and 1.0 slopes, respectively (Figure S1 in the Supporting Information), indicating that the evolution of the polarizability along the series is mainly determined by the heteroatom, with the contribution of the *cis*-butadienic moiety to the polarizability of the heterocycle being almost constant. Similar relationships have been previously reported in the furan⁵⁵ and cyclopentadiene⁵⁴ homologue series. We note that the present $\langle\alpha^e\rangle$ values are $\sim 2-4$ times larger than those of the corresponding hydrides.

Electronic polarizabilities have often been related to the molecular hardness, η , a useful parameter that provides indications on the stability of a molecular system.⁵⁶ The parameter η is usually expressed as $\eta \sim (IP - EA)/2 \sim (\epsilon_{LUMO} - \epsilon_{HOMO})/2$, where IP, EA, ϵ_{LUMO} , and ϵ_{HOMO} are the ionization potential, electron affinity, and the LUMO and HOMO eigenvalues, respectively. The ϵ_{LUMO} and ϵ_{HOMO} values were computed at the B3LYP level using the ECP basis set CEP-31G of Stevens et al.,⁵⁷ since, for pyrrole, the LUMO is incorrectly predicted to be of a_1 (σ^*) symmetry by the Pol basis set. Vertical B3LYP/Pol IP and EA values were evaluated through a Δ SCF procedure as the energy difference between the neutral ground and the lowest ionic state, using the optimized geometry of the neutral ground state. In all the molecules, the HOMO (a_2 or a'' type orbital; see Figure S2 in the Supporting Information) is localized in the *cis*-butadienic moiety. For pyrrole, the LUMO has b_1 symmetry and is characterized by a substantial overlap between the lone-pair of the heteroatom and the π^* orbital of the *cis*-butadienic fragment, whereas, for the heavier homologues, it (a' symmetry) shows a weaker interaction between the π^* orbital of the *cis*-butadienic moiety and the σ^* orbital of the exocyclic H-X bond. The B3LYP/Pol IP value of pyrrole (2A_2) is 8.25 eV, in excellent agreement with the observed value of 8.21 eV,⁵⁸ while the corresponding EA datum (2B_1) computed at -1.60 eV overestimates the experimental value of -2.36 eV.⁵⁹ Experimental IP and EA values of the heavier homologues are unknown. The results show that, in passing from pyrrole to

TABLE 3: Dipole Moments (au) and Electronic Dipole (Hyper)polarizabilities (au) for the Transition State (C_{2v}) of C_4H_4XH (X = P, As, Sb, Bi)^a

	C_4H_4PH	C_4H_4AsH	C_4H_4SbH	$C_4H_4BiH^b$
μ	0.538	0.529	0.508	0.487
$\langle\alpha\rangle$	74.95	81.41	98.08	106.67
β_{vec}	146.8	206.8	416.0	604.9
$\langle\gamma\rangle$	31690	36015	57828	76473

^a Calculations were carried out at the MP2/Pol level on the B3LYP/Pol geometry. ^b Calculations were carried out at the MP2/ECP-Pol level on the B3LYP/ECP-Pol geometry.

phosphole, the IP value increases from 8.25 to 8.73 eV and then decreases uniformly down the group (8.69, 8.61, and 8.53 eV for arsole, stibole, and bismole, respectively). On the other hand, the EA increases monotonically as the heteroatom becomes heavier (-1.60, -0.37, -0.29, -0.10, and -0.05 eV for pyrrole, phosphole, arsole, stibole, and bismole, respectively), with the datum of bismole being close to zero. As a result, the η value decreases monotonically along the series (the most noticeable variation being found between pyrrole and phosphole), consistent with the linear relationship between the polarizability increase, $\langle\alpha^e\rangle$, and the $1/\eta$ values for C_4H_4XH (X = P, As, Sb, Bi) ($r^2 = 1.00$) (Figure S3 in the Supporting Information). This result suggests that η is a useful parameter to determine the evolution of the polarizabilities along this series of molecules. Note also that η and the calculated atomization energy are linearly related ($r^2 = 0.99$), confirming that the ring stability decreases along the series.

Besides the effect of the heavy atom substitution, the electronic (hyper)polarizabilities are significantly enhanced by the increase in the π conjugation. Previous calculations on series of π -conjugated molecules indicated that the electronic (hyper)polarizabilities increase with decreasing the C-C bond length alternation.⁶⁰ In Table 3, the static electronic polarizabilities of the planar form of C_4H_4XH (X = P, As, Sb, Bi) are given. The comparison between the data of Tables 1 and 3 reveals that, in passing from the planar to the pyramidal structure, the $\langle\alpha^e\rangle$ values decrease by 4-12%. The noted decrease in the values of polarizabilities is consistent with the relative stability increase, thus the minimum polarizability principle,⁶¹ which states that any system should proceed toward a state of minimum polarizability, is satisfied. By contrast, recent B3LYP calculations with split valence plus polarization basis sets (SV(P)) on a series of oligophospholes, including the monomer, have predicted $\langle\alpha^e\rangle(\text{planar}) < \langle\alpha^e\rangle(\text{pyramidal})$ for all investigated oligomers.¹¹

It is of interest to compare the electronic polarizabilities of the present molecules (group 15) with those of the cyclopentadiene (group 14)⁶² and furan (group 16)⁵⁵ homologue series. The B3LYP/Pol $\langle\alpha^e\rangle$ values for $C_4H_4CH_2$, $C_4H_4SiH_2$, $C_4H_4GeH_2$, and $C_4H_4SnH_2$ are 59.32, 73.67, 77.44, and 87.50 au, respectively, whereas the corresponding values for C_4H_4O , C_4H_4S , C_4H_4Se , and C_4H_4Te ⁵⁵ are 49.71, 65.46, 72.45, and 86.59

au, respectively. These results show that the electronic dipole polarizability values follow the order $\langle\alpha^e\rangle(\text{group 16}) < \langle\alpha^e\rangle(\text{group 15}) \sim \langle\alpha^e\rangle(\text{group 14})$, in substantial agreement with previous MP2/6-31+G(d,p)¹⁰ and B3LYP/SV(P)¹¹ calculations on $\text{C}_4\text{H}_4\text{X}$ ($\text{X} = \text{O}, \text{S}, \text{NH}, \text{PH}, \text{CH}_2, \text{SiH}_2$) systems. A notable exception is found for the smallest homologues, where $\langle\alpha^e\rangle(\text{pyrrole}) < \langle\alpha^e\rangle(\text{cyclopentadiene})$. The above trend is essentially dominated by the polarizability of the X fragments, which, according to HF/Pol computations monotonically increases in the order $\alpha_{\text{X}}(\text{group 16}) < \alpha_{\text{XH}}(\text{group 15}) < \alpha_{\text{XH}_2}(\text{group 14})$.^{23–25} In addition, the different aromatic character for the three series of heterocycles, as expressed by thermodynamic stability factors inside the ring, also seems to be effective. Indeed, by following previous calculations for the energy for the bond separation, isodesmic, homodesmotic, and superhomodesmotic reactions for five-membered heterocycles $\text{C}_4\text{H}_4\text{X}$ ($\text{X} = \text{O}, \text{S}, \text{Se}, \text{Te}, \text{NH}, \text{PH}, \text{AsH}, \text{SbH}, \text{CH}_2, \text{SiH}_2, \text{GeH}_2$),^{19,63} the thermodynamic stability (aromaticity) decreases in the order group16 > group 15 > group14, except for the couple furan–pyrrole, where the order is reversed.

3.4. Electronic First Dipole Hyperpolarizabilities. The static electronic first dipole hyperpolarizabilities of the pyrrole homologues are listed in Table 1. Experimental β^e values of these molecules are not known. Our best static β_{vec}^e values (CCSD(T)) are 44.0, 74.3, 122.3, 265.0, and 406.9 au for pyrrole, phosphole, arsole, stibole, and bismole, respectively. Except for phosphole, β_z^e dominates the first hyperpolarizability in the series, the β_z^e/β_x^e ratio increases as the heteroatom becomes heavier, and the CCSD(T) values are 0.69, 1.36, 1.90, and 2.61, in phosphole, arsole, stibole, and bismole, respectively. For pyrrole electron correlation, effects introduced by ab initio methods are substantial, and the CCSD(T)/Pol β_{vec}^e value increases with respect to the HF/Pol datum by 60%, whereas, for the heavier homologues, it increases by 2–16%, with the smaller percentage being found for bismole. MP2 β_{vec}^e values are in fair agreement with those obtained at the CCSD(T) level, whereas, between the DFT methods, the PBE1PBE functional provides a better performance. It is worth noting that, in a different way to $\langle\alpha^e\rangle$, the basis set effect on β_{vec}^e is much more important. Indeed, at the correlated level, the β_{vec}^e values increase by 8–15% in passing from the Pol to the ECP–Pol basis set, indicating moderate relativistic corrections; they do not, however, alter the β_{vec}^e order along the series.

Dynamic β^e calculations have been performed at the HF/Pol//B3LYP/Pol level for the second harmonic generation (SHG; $\beta^e(-2\omega; \omega, \omega)$) and the electrooptical Pockel effect (EOPE; $\beta^e(-\omega; \omega, 0)$) NLO processes in the range $\hbar\omega = 0–0.072$ au. As expected, $\beta_{\text{vec}}^e(-2\omega; \omega, \omega) > \beta_{\text{vec}}^e(-\omega; \omega, 0)$ in all the molecules. By analogy to $\langle\alpha^e\rangle(\omega; \omega)$, frequency-dependent β_{vec}^e values have been expressed as an even-order power-series expansion of ω truncated to the fourth order:⁵⁰

$$\beta_{\text{vec}}^e(-\omega_\sigma; \omega_1, \omega_2) = \beta_{\text{vec}}^e(0; 0, 0) [1 + A''\omega_L^2 + B''\omega_L^4] \quad (7)$$

where $\omega_\sigma = \omega_1 + \omega_2$ and $\omega_L^2 = \omega_1^2 + \omega_2^2 + \omega_\sigma^2$. Both the A'' and B'' expansion coefficients obtained for the EOPE and SHG processes in the $\hbar\omega = 0.0–0.042$ au range are summarized in Table 2. In agreement with theoretical predictions,⁶⁴ for any given molecule, the A'' value is constant within 1% for both NLO processes, while, except for pyrrole, B'' value varies by 6–15%. Both the A'' and B'' terms increase with the atomic number of the heteroatom, as previously noticed in the furan homologue series.⁵³ At a wavelength of 790 nm ($\hbar\omega = 0.058$ au), sufficiently far from the electronic resonance with the lowest

excitation energy, which has been found experimentally for pyrrole at 5.86 eV (0.22 au),⁶⁵ the dispersion correction of $\beta_{\text{vec}}^e(-2\omega; \omega, \omega)$ for pyrrole, phosphole, arsole, stibole, and bismole amounts to 11, 27, 30, 38, and 42% of the static value, respectively. As expected, the corresponding data for the EOPE process are smaller, that is, 5, 8, 9, 11, and 12%, respectively. By contrast, previous TDHF/4-31G+pd calculations on pyrrole at $\lambda = 602$ nm gave an analogous dispersion correction for both the SHG and the EOPE processes (2.5%).⁹ It is worth noting that the dispersion effects in the present molecules are somewhat greater than those previously obtained in the furan homologue series, which, for the SHG and EOPE processes at $\lambda = 790$ nm, are within 4–30% and 1–4%, respectively.⁵³

At all the levels of calculation, similar to $\langle\alpha^e\rangle$, β_{vec}^e shows a monotonic increment along the series. Note that the substitution of nitrogen by bismuth leads to a β_{vec}^e increase of ~ 1 order of magnitude. Present β_{vec}^e values are linearly correlated with those of the hydrides XH_3 (at the HF/POL level, the β_{vec}^e values are 0.1, 20.5, 21.7, 83.2, and 117.4 au for NH_3 , PH_3 , AsH_3 , SbH_3 , and BiH_3 , respectively) ($r^2 = 0.99$) with a line slope of 3 (Figure S4 in the Supporting Information), which gives evidence of the effect of the *cis*-butadienic moiety in enhancing the first electronic dipole hyperpolarizability. Furthermore, the β_{vec}^e value increases as the calculated η value decreases, and a linear relationship is established between the β_{vec}^e and $1/\eta$ values of $\text{C}_4\text{H}_4\text{XH}$ ($\text{X} = \text{P}, \text{As}, \text{Sb}, \text{Bi}$) ($r^2 = 0.99$).

As expected, for all the molecules, the increase in the π conjugation noticeably enhances the first dipole hyperpolarizability, and the MP2 β_{vec}^e values of the planar form (Table 3) are larger than those of the pyramidal structure (Table 1) by 50–90%. These percentages are considerably greater than those found for $\langle\alpha^e\rangle$.

The static β^e values of the pyrrole homologues may be compared with the corresponding ones of the furan⁵⁵ and cyclopentadiene⁶² homologue series. The B3LYP/Pol β_{vec}^e values are 17.8, 20.3, 61.4, and 149.4 au for $\text{C}_4\text{H}_4\text{CH}_2$, $\text{C}_4\text{H}_4\text{SiH}_2$, $\text{C}_4\text{H}_4\text{GeH}_2$, and $\text{C}_4\text{H}_4\text{SnH}_2$,⁶² respectively, and 41.7, 21.8, 74.6, and 219.4 au for $\text{C}_4\text{H}_4\text{O}$, $\text{C}_4\text{H}_4\text{S}$, $\text{C}_4\text{H}_4\text{Se}$, and $\text{C}_4\text{H}_4\text{Te}$,⁵⁵ respectively. One notices that, except for the lightest homologues, where $\beta_{\text{vec}}^e(\text{furan}) > \beta_{\text{vec}}^e(\text{pyrrole}) \sim \beta_{\text{vec}}^e(\text{cyclopentadiene})$, the β_{vec}^e value of the pyrrole homologue is always greater than the corresponding value in the furan and cyclopentadiene homologue series. This is particularly evident for phosphole, whose β_{vec}^e value is predicted to be ~ 4 times larger than that of both thiophene⁵⁵ and silole,⁶² in substantial agreement with the results obtained by Hinchliffe and Soscun Machado¹⁰ at the HF/6-31+(3df,3pd) level.

3.5. Electronic Second Dipole Hyperpolarizabilities. Table 1 reports the static electronic $\langle\gamma^e\rangle$ values of the investigated molecules. As far as we know, experimental γ^e values are not available. At the highest level of theory, CCSD(T), the static $\langle\gamma^e\rangle$ values are calculated to be 18838, 23027, 25696, 35874, and 39306 au for pyrrole, phosphole, arsole, stibole, and bismole, respectively. Specifically, in passing from pyrrole to phosphole and bismole, the CCSD(T) $\langle\gamma^e\rangle$ value increases by ~ 20 and 100%, respectively. Electron correlation effects to $\langle\gamma^e\rangle$ are positive, with the CCSD(T) corrections amounting to 15–20% of the HF values. MP2 $\langle\gamma^e\rangle$ values are in reasonable agreement with the CCSD(T) results within 2–8%, while, between employed functionals, PBE1PBE better reproduces the CCSD(T) data. For pyrrole, the present HF/Pol $\langle\gamma^e\rangle$ value is in good agreement with the previous estimate of El-Bakali-Kassimi

et al.⁷ obtained by TDHF/4-31G+pd calculations (16380 au). More recently, Jug et al.⁸ reported some $\langle\gamma^e\rangle$ estimates of pyrrole using the LDA functional with the TZVP+FIP basis set. Their best $\langle\gamma^e\rangle$ value of 25935 au compares well with our correlated values, especially with the DFT data. For the heavier homologues, because of relativistic contributions, the basis set effect on $\langle\gamma^e\rangle$ is not uniform: as expected, it is small (1–2%) for C₄H₄XH (X = P, As, Sb) while being more pronounced for bismole, where the ECP–Pol basis set provides $\langle\gamma^e\rangle$ values smaller than those obtained with the Pol basis set by 7–8%. The last behavior is somewhat different from that recently observed on HI,³² H₂Po,³² and C₄H₄Te³³ molecules, where, in passing from the Pol to the ECP–Pol basis set, $\langle\gamma^e\rangle$ values increase. However, it must be noted that the introduction of the approximate relativistic ECP corrections does not modify the $\langle\gamma^e\rangle$ order along the present series of molecules.

The frequency dependence of γ^e has been evaluated at the HF/Pol/B3LYP/Pol level for the third harmonic generation (THG; $\gamma^e(-3\omega;\omega,\omega,\omega)$), electric field-induced second harmonic generation (EFISH; $\gamma^e(-2\omega;\omega,\omega,0)$), intensity-dependent refractive index (IDRI; $\gamma^e(-\omega;\omega,\omega,-\omega)$) and the dc-Kerr effect (dc-KE, $\gamma^e(-\omega;\omega,0,0)$) NLO processes in the $\hbar\omega$ range of 0–0.072 au. In all the molecules, as expected, the dynamic $\langle\gamma^e\rangle$ values follow the order $\gamma^e(-3\omega;\omega,\omega,\omega) > \gamma^e(-2\omega;\omega,\omega,0) > \gamma^e(-\omega;\omega,\omega,-\omega) > \gamma^e(-\omega;\omega,0,0)$. Similar to that for the dynamic α^e and β^e data, the frequency-dependent γ^e values for the THG, EFISH, IDRI, and dc-KE processes have been expressed as⁵⁰

$$\langle\gamma^e\rangle(-\omega_\sigma;\omega_1,\omega_2,\omega_3) = \langle\gamma^e\rangle(0;0,0,0) [1 + A'''\omega_L^2 + B'''\omega_L^4] \quad (8)$$

where $\omega_\sigma = \omega_1 + \omega_2 + \omega_3$, $\omega_L^2 = \omega_1^2 + \omega_2^2 + \omega_3^2 + \omega_\sigma^2$, and A''' and B''' are the second-order and fourth-order expansion coefficients, respectively. As the incident optical $\hbar\omega$ approaches 0.072 au (1.96 eV), the THG data show substantial resonant contributions because $3\hbar\omega$ is close to the experimental lowest excitation energy of pyrrole (5.86 eV).⁶⁵ Thus, we evaluated A''' and B''' values in the $\hbar\omega$ range of 0–0.035 au (Table 2). Both A''' and B''' coefficients decrease in passing from pyrrole to phosphole, remaining almost constant for phosphole and arsole and then increasing in the heavier homologues. In substantial agreement with theoretical predictions,⁶⁴ the A''' value for all the NLO processes remains constant within 3%, while the B''' coefficient for the SHG and IDRI processes is the same within 2%. At the $\hbar\omega$ value of 0.058 au ($\lambda = 790$ nm), the dispersion correction to $\langle\gamma^e\rangle$ for the IDRI process amounts to 32, 26, 26, 31, and 34% of the static value for pyrrole, phosphole, arsole, stibole, and bismole, respectively. This is somewhat larger than those previously obtained in the furan⁶⁶ and cyclopentadiene⁵⁴ homologue series, which are within 11–14% and 22–26%, respectively. Previously, TDHF/4-31G+pd calculations on pyrrole at $\lambda = 602$ nm gave a dispersion correction for the $\gamma^e(-\omega;\omega,\omega,-\omega)$ value of 42%,⁹ to be compared, by using eq 4, with the present TDHF/Pol value of 48%.

At all the levels of theory, the $\langle\gamma^e\rangle$ value increases monotonically as the heteroatom becomes heavier, and, likewise, for $\langle\alpha^e\rangle$ and β_{vec}^e , a linear relationship exists between the $\langle\gamma^e\rangle$ (C₄H₄XH) and $\langle\gamma^e\rangle$ (XH₃) values (at the HF/POL level, the $\langle\gamma^e\rangle$ values are 3092, 7037, 8865, 15453, and 19796 au for NH₃, PH₃, AsH₃, SbH₃, and BiH₃, respectively) ($r^2 = 0.98$) with unit slope (Figure S5 in the Supporting Information). This result suggests that, analogous to $\langle\alpha^e\rangle$ and β_{vec}^e , the electronic second dipole

hyperpolarizability of the investigated molecules is almost exclusively dominated by the heteroatom, as previously observed in the furan⁶⁶ and cyclopentadiene⁵⁴ homologue series. It is of interest to note that the $\langle\gamma^e\rangle$ values of the present molecules are ~2–5 times higher than those of the corresponding hydrides. Furthermore, the increase in $\langle\gamma^e\rangle$ along the series is consistent with the decrease in η in the same order, with the $\langle\gamma^e\rangle$ and $1/\eta$ values of C₄H₄XH (X = P, As, Sb, Bi) being in a good linear relationship ($r^2 = 0.99$), confirming once more that the evolution of the electronic properties along the group attests to a molecular stability reduction. A similar relationship was also observed in the furan homologue series.⁶⁶

Likewise, for β_{vec}^e and, to a lesser extent, $\langle\alpha^e\rangle$, the increase in the π conjugation due to ring planarization leads to a remarkable enhancement of the electronic second dipole hyperpolarizability. Upon proceeding from the pyramidal to the planar structure, the MP2 $\langle\gamma^e\rangle$ values increase by 30–90% (compare the results in Tables 1 and 3).

Present static $\langle\gamma^e\rangle$ values are compared with the corresponding data of the cyclopentadiene⁵⁴ and furan⁶⁶ homologue series for which experimental $\gamma^e(-\omega;\omega,\omega,-\omega)$ values at $\lambda = 790$ nm ($\hbar\omega = 0.058$ au) are known.⁶⁷ B3LYP/Pol $\langle\gamma^e\rangle$ values are 20395, 24046, 25130, and 31338 au for C₄H₄CH₂, C₄H₄SiH₂, C₄H₄GeH₂, and C₄H₄SnH₂,⁵⁴ respectively, and 15573, 20416, 24003, and 35078 au for C₄H₄O, C₄H₄S, C₄H₄Se, and C₄H₄Te,⁶⁶ respectively. The results show that the $\langle\gamma^e\rangle$ values of the pyrrole homologues are always higher than those of the cyclopentadiene and furan series by 8–21% and 12–30%, respectively. These percentages are expected to increase further for the corresponding frequency-dependent $\langle\gamma^e\rangle$ values. We note that this trend is consistent with the calculated $1/\sqrt{A'}$ values, which are smaller in the group 15 homologues, whereas it cannot be rationalized on the basis of atomic contributions. In fact, by following the previous HF results reported by Stiehler and Hinze⁶⁸ for C, N, O, Si, P, S, Ge, As, and Se atoms, $\langle\gamma^e\rangle$ invariably increases from group 16 to group 15 and then to group 14. Thus, the role provided by other factors such as thermodynamic stability and π -conjugation in the ring seems to be crucial to establish the trend in the $\langle\gamma^e\rangle$ values of the five-membered heterocyclic homologue series.

3.6. Vibrational Contributions. The computed vibrational contributions, PV and ZPVA, of C₄H₄XH (X = N, P, As, Sb) are summarized in Table 4. Generally, the ZPVA contributions are small in comparison with the electronic terms, being less than 5% for α and γ , up to 10% for β , and less than 1% for μ (not shown). Thus, with the possible exception of β , the ZPVA contributions are negligible for those dipolar properties, which involve only optical frequencies, in which the PV contributions are generally negligible, too.

For the static PV contributions, we first note that the influence of electronic correlation, as computed at the MP2 level, is quite small on the α^{PV} and β^{PV} of pyrrole and the α^{PV} of phosphole and arsole in the double-harmonic approximation, but is quite large on the β^{PV} of phosphole, and smaller, but still appreciable on the β^{PV} for arsole.

The static PV contributions behave quite differently for the planar C₄H₄NH and the nonplanar molecules C₄H₄XH, with X = P, As, and Sb. For all the molecules, there is only a small difference between the components of α^{PV} at the double-harmonic level (sum of the electrical and mechanical anharmonicities = 0) and the higher perturbational level, where the total sum of the electrical and mechanical anharmonicities included is 2. This is also valid for the computed terms of the β^{PV} and, to a lesser extent, the γ^{PV} of C₄H₄XH, with X = P,

TABLE 4: Static PV and ZPVA Contributions to the (Hyper)polarizabilities (au) of C₄H₄XH (X = N, P, As, Sb)^a

	$\langle\alpha\rangle$	β_{zzz}	β_{xxz}	β_{vec}	γ_{xxxx}	γ_{yyyy}	γ_{zzzz}	γ_{xxzz}	$\langle\gamma\rangle$
C ₄ H ₄ NH									
PV/SCF/43210 ^b	6.89	-34.32	-630.1	398.27	-22316	4605	2668	82413	29933
PV/SCF/DH ^c	7.25	-4.93	51.98	28.85	-120	4125	3485	-794	1468
PV/MP2/DH ^c	6.65	3.42	49.06	33.04					
ZPVA/SCF	1.65	1.69	0.53	1.35	-5	294	308	30	183
C ₄ H ₄ PH									
PV/SCF/43210 ^b	3.27	111.52	-62.08	50.63	3720	6201	7947	2342	5517
PV/SCF/DH ^c	3.22	110.93	-66.18	36.33	2290	5163	7409	1381	4334
PV/MP2/DH ^c	4.19	214.65	-95.09	82.96					
ZPVA/SCF	1.87	4.08	-2.61	2.61	-107	327	211	91	154
C ₄ H ₄ AsH									
PV/SCF/43210 ^b	3.42	93.98	-74.54	78.45	5764	6888	6750	3545	6661
PV/SCF/DH ^c	3.36	99.92	-75.06	56.52	3069	5682	7475	2732	5426
PV/MP2/DH ^c	3.59	133.08	-102.20	40.83					
ZPVA/SCF	1.92	5.76	-1.26	2.44	-68	328	277	71	170
C ₄ H ₄ SbH ^d									
PV/SCF/32222 ^e	5.57	163.88	-72.95	143.16	14896	7247	11471	6503	12420
PV/SCF/DH ^c	5.08	143.49	-65.18	118.93	6490	5309	8832	4465	8067
ZPVA/SCF	2.16	9.08	-3.67	4.40	645	1242	1869	406	1146

^a Calculations were carried out on the equilibrium geometry with the 6-311G** basis set. ^b Property derivatives of order $mnpq = 43210$. ^c Double-harmonic approximation. ^d Calculations were carried out on the equilibrium geometry with the Pol basis set. ^e Property derivatives of order $mnpq = 32222$.

As, and Sb. The components at the higher perturbational level are up to a factor of 2 larger than those at the double-harmonic level. We note that the apparently higher effect on the γ^{PV} of C₄H₄SbH may be due to the smaller order of derivatives included in the computation for this molecule as compared to the other molecules ($mnpq = 32222$ versus $mnpq = 43210$). Test calculations for C₄H₄XH, with X = P and As with the reduced set of derivatives $mnpq = 32210$, show that the fourth-order derivative of the energy ($m = 4$) and the third-order derivative of the dipole ($n = 3$) generally *decrease* the computed components of β^{PV} and γ^{PV} . Thus, it is conceivable that the β^{PV} and γ^{PV} of C₄H₄SbH, computed with derivatives of order $mnpq = 43210$ would be smaller than those computed here and therefore closer to those at the double-harmonic level. Note that the derivatives of γ ($p = 1,2$) do not contribute to β^{PV} and γ^{PV} at the level of anharmonicities considered. Additionally, test calculations show that the second derivative of β ($p = 2$) has a small influence on γ^{PV} .

The situation is quite different for C₄H₄NH: for this molecule, some of the components of β^{PV} and γ^{PV} at the double-harmonic level differ by orders of magnitude from those computed with $mnpq = 43210$; this specifically affects the components β_{xxz}^{PV} , γ_{xxxx}^{PV} , γ_{xxzz}^{PV} . This was already noted and analyzed in more detail in ref 8, where it was shown that, for β^{PV} , the anharmonicity level I and, for γ^{PV} , the anharmonicity level II are responsible for the largest contributions to the respective components.

It may be of interest to identify the normal modes responsible for the large PV contributions. We can identify the normal mode with the lowest frequency, computed to be at 490 cm⁻¹, as the reason for the large PV contributions: without this mode, we find $\beta_{xxz}^{PV} = 6.8$ au, $\gamma_{xxxx}^{PV} = 1850$ au, and $\gamma_{xxzz}^{PV} = 1118$ au, in contrast to the values of $\beta_{xxz}^{PV} = -630$ au, $\gamma_{xxxx}^{PV} = -22316$ au, and $\gamma_{xxzz}^{PV} = 82413$ au when it is included. The influence of this normal mode on the other components, which are, in any case, much smaller in absolute terms, is rather small in comparison. The mode in question corresponds to an out-of-plane wagging motion of the N-H group, with an appreciably large contribution to the IR spectrum (intensity = 104.2 km/mol; about 20% with respect to the mode with the largest intensity, which occurs at $\nu = 820$ cm⁻¹). This suggests that it is the first derivative of the dipole moment that may be responsible for the large PV

values. This is, in fact, shown to be the case when these derivatives are removed from the set of derivatives used for the calculations. This again reduces the two large components γ_{xxxx}^{PV} and γ_{xxzz}^{PV} by several orders of magnitude, while the other components of γ^{PV} are much less affected. In accordance with the recent work of Torrent-Succarrat et al.,⁴⁰ our findings raise the question of whether the perturbation series is convergent at all for the γ^{PV} of pyrrole and, thus, whether any significance can be assigned to the computed values of this property. Different computational techniques employing the vibrational self-consistent field method,⁶⁹ which are not yet available in standard packages and may also be difficult to use for systems as large as pyrrole, have to be applied to answer this question. We also note that the complete computation of β^{PV} and γ^{PV} at the anharmonicity level II requires additional derivatives not available here (third-order derivatives of β and α),³⁶ and the influence of those terms on the computed values are not known.

It is noteworthy that the similar normal mode consisting mainly of the out-of-plane wagging motion of the X-H group in the other molecules corresponds to even lower frequencies than those in the case of pyrrole: 350 cm⁻¹ for C₄H₄PH, 314 cm⁻¹ for C₄H₄AsH, and 283 cm⁻¹ for C₄H₄SbH. Thus, one could expect similarly large or even larger PV contributions for these molecules due to this mode. However, the influence of the decreasing frequency is apparently more than counterbalanced by the decrease in the corresponding first dipole derivatives, as shown by the decreasing IR intensity of this mode in the series (N: 104.2, P: 5.32, As: 2.09, Sb: 0.98 km/mol).

We also note that, at the MP2 level, both the frequencies of the wagging mode increase and the IR intensity decreases: we find N: 440 cm⁻¹, 68.2 km/mol; P: 316.2 cm⁻¹, 10.53 km/mol, and As: 275.8 cm⁻¹, 4.09 km/mol. Both effects are likely to decrease the contribution of this mode to the PV contributions. Thus, it is possible that the large PV contributions of some components of the β^{PV} and γ^{PV} of pyrrole found at the SCF level are strongly reduced at the correlated MP level.

4. Summary

In this work, we have determined the structures, barriers to inversion at the heteroatom, and the electronic and vibrational

(hyper)polarizabilities of the pyrrole homologues C_4H_4XH ($X = N, P, As, Sb, Bi$) using ab initio HF, MP2, CCSD, CCSD(T), as well as DFT B3LYP and PBE1PBE methods with the Sadlej's Pol and 6-311G** basis sets. The results have shown that the static and frequency-dependent electronic properties monotonically increase with the atomic number of the heteroatom, consistent with the decreases in the molecular hardness. The relativistic effects are small for α^e , while they are more important for μ , β^e , and γ^e values. The pyramidalized equilibrium structure of C_4H_4XH ($X = P, As, Sb, Bi$) is less polarizable than the planar one by 4–12%, consistent with the minimum polarizability principle. The effects of the ring planarization are especially conspicuous on the β_{vec}^e and $\langle \gamma^e \rangle$ values, which are enhanced with respect to the pyramidalized structure by 50–90% and 30–90%, respectively. The electronic hyperpolarizabilities of the pyrrole homologues are higher than the corresponding ones in the furan and cyclopentadiene homologue series, except for the lightest homologues, where $\beta_{\text{vec}}^e(C_4H_4O) > \beta_{\text{vec}}^e(C_4H_4NH) \sim \beta_{\text{vec}}^e(C_4H_4CH_2)$. These results suggest that oligomers and polymers based on the pyrrole homologue units are potential candidates as organic NLO materials and present an alternative to the furan and cyclopentadiene homologues. Vibrational terms are important contributors to the total (hyper)polarizability. ZPVA terms are predicted to be smaller than the PV counterparts. Anharmonic corrections dominate the β^{PV} and γ^{PV} values of pyrrole, where the most contributing mode originates from the low-frequency out-of-plane wagging vibration, in agreement with the results of ref 8. For the heavier homologues, the anharmonic effects are less important, where the double-harmonic terms give the larger contributions to the vibrational hyperpolarizabilities.

Acknowledgment. A.A. thanks MIUR, Rome for partial support.

Supporting Information Available: Seven tables listing structural parameters (Table S1), inversion barriers (Table S2), and dipole moment and (hyper)polarizability data (Tables S3–S7). Five figures depicting property relationships (Figures S1 and S3–S5) and a molecular orbitals plot (Figure S2). This material is available free of charge via the Internet at <http://pubs.acs.org>.

References and Notes

- Prasad, P. N.; Williams, D. J. *Introduction to Nonlinear Optical Effects in Molecules and Polymers*; Wiley: New York, 1991. Nalwa, H. S.; Miyata, S. *Nonlinear Optics of Organic Molecules and Polymers*; CRC Press: Boca Raton, FL, 1997.
- Diaz, A. F.; Kanazawa, K. K.; Gardini, G. P. *J. Chem. Soc., Chem. Commun.* **1988**, 183. Waltman, R. J.; Bargon, J.; Diaz, A. D. *J. Phys. Chem.* **1983**, *87*, 1459. Thienpont, H.; Rikken, G. L. J. A.; Meijer, E. W.; ten Hoeve, W.; Wynberg, H. *Phys. Rev. Lett.* **1990**, *65*, 2141. Worland, R.; Phillips, S. D.; Walker, W. C.; Heeger, A. J. *Synth. Met.* **1989**, *28*, D669.
- Ghoshal, S. K. *Chem. Phys. Lett.* **1989**, *158*, 65.
- Samuelson, L. A.; Druy, M. A. *Macromolecules* **1986**, *19*, 824.
- Le Fevre, C. G.; Le Fevre, R. J. W.; Rao, B. P.; Smith, M. R. *J. J. Chem. Soc.* **1959**, 1188.
- Calderbank, K. E.; Calvert, R. L.; Lukins, P. B.; Ritchie, G. L. P. *Aust. J. Chem.* **1981**, *34*, 1835.
- El-Bakali Kassimi, N.; Doerksen, R. J.; Thakkar, A. J. *J. Phys. Chem.* **1996**, *100*, 8752.
- Jug, K.; Chiodo, S.; Calaminici, P.; Avramopoulos, A.; Papadopoulos, M. G. *J. Phys. Chem. A* **2003**, *107*, 4172.
- Keshari, V.; Wijekoon, W. M. K. P.; Prasad, P. N.; Karna, S. P. *J. Phys. Chem.* **1995**, *99*, 9045.
- Hinchliffe, A.; Soscun Machado, H. J. *J. Mol. Struct. (THEOCHEM)* **1995**, *331*, 109.
- Delaere, D.; Nguyen, M. T.; Vanquickenborne, L. G. *Phys. Chem. Chem. Phys.* **2002**, *4*, 1522.
- Toto, J. L.; Toto, T. T.; de Melo, C. P.; Robins, K. A. *J. Chem. Phys.* **1995**, *102*, 8048. Otto, P.; Martinez, A.; Czaja, A.; Ladik, J. *J. Chem. Phys.* **1992**, *117*, 1908.
- Albert, I. D. L.; Marks, T. J.; Ratner, M. A. *J. Am. Chem. Soc.* **1997**, *119*, 6575.
- Mathey, F. *Chem. Rev.* **1988**, *88*, 429. Mathey, F. In *Phospholes in Science of Synthesis*; Maas, G., Ed.; Thieme: Stuttgart, Germany, 2001; p 553. Quin, L. D. In *Phospholes in Phosphorus–Carbon Heterocyclic Chemistry: The Rise of a New Domain*; Mathey, F., Ed.; Elsevier: Oxford, 2001; p 219.
- Fave, C.; Cho, T.-Y.; Hissler, M.; Chen, C.-W.; Luh, T.-Y.; Wu, C.-C.; Réau, R. *J. Am. Chem. Soc.* **2003**, *125*, 9254.
- Coggon, P.; Engel, J. F.; McPhail, A. T.; Quin, L. D. *J. Am. Chem. Soc.* **1970**, *92*, 5779. Coggon, P.; McPhail, A. T. *J. Chem. Soc., Dalton Trans.* **1973**, 1988.
- Egan, W.; Tang, R.; Zon, G.; Mislow, K. *J. Am. Chem. Soc.* **1970**, *92*, 1442. Egan, W.; Tang, R.; Zon, G.; Mislow, K. *J. Am. Chem. Soc.* **1971**, *93*, 6205.
- Nyulási, L.; Soos, L.; Keglevich, G. *J. Organomet. Chem.* **1998**, *566*, 29 and references therein.
- Baldrigge, K. K.; Gordon, M. S. *J. Am. Chem. Soc.* **1988**, *110*, 4204.
- Berger, D. J.; Gaspar, P. P.; Liebman, J. F. *J. Mol. Struct. (THEOCHEM)* **1995**, *338*, 51.
- Pelzer, S.; Wichmann, K.; Wesendrup, R.; Schwerdtfeger, P. *J. Phys. Chem. A* **2002**, *106*, 6387.
- Champagne, B.; Luis, J. M.; Duran, M.; Andrés, J. L.; Kirtman, B. *J. Chem. Phys.* **2000**, *112*, 1011.
- Sadlej, A. *J. Collect. Czech. Chem. Commun.* **1988**, *53*, 1995. Sadlej, A. *J. Theor. Chim. Acta* **1991**, *79*, 123. Sadlej, A. *J. Theor. Chim. Acta* **1991**, *81*, 45.
- Sadlej, A. *J. Theor. Chim. Acta*, **1992**, *81*, 339.
- Sadlej, A. *J. Theor. Chim. Acta*, **1992**, *83*, 351.
- Sekino, H.; Bartlett, R. J. *J. Chem. Phys.* **1986**, *85*, 976. Karna, S. P.; Dupuis, M. *J. Comput. Chem.* **1991**, *12*, 487.
- Perdew, J. P.; Burke, K.; Ernzerhof, M. *Phys. Rev. Lett.* **1997**, *78*, 1396.
- Kurtz, H. A.; Stewart, J. J. P.; Dieter, K. M. *J. Comput. Chem.* **1990**, *11*, 82.
- Chopra, P.; Carlucci, L.; King, H. F.; Prasad, P. N. *J. Phys. Chem.* **1989**, *93*, 7120. Sim, F.; Chin, S.; Dupuis, M.; Rice, J. E. *J. Phys. Chem.* **1993**, *97*, 1158.
- Avramopoulos, A.; Reis, H.; Li, J.; Papadopoulos, M. G. *J. Am. Chem. Soc.* **2004**, *126*, 6179 and references therein.
- Papadopoulos, M. G.; Reis, H.; Avramopoulos, A.; Erkoç, S.; Amirouche, L. *J. Phys. Chem. B* **2005**, *109*, 18822 and references therein.
- Norman, P.; Schimmelpfennig, B.; Ruud, K.; Jensen, H. J. Aa.; Ågren, H. *J. Chem. Phys.* **2002**, *116*, 6914.
- Jansik, B.; Schimmelpfennig, B.; Norman, P.; Macak, P.; Ågren, H.; Ohta, K. *J. Mol. Struct. (THEOCHEM)* **2003**, *633*, 237.
- Bergner, A.; Dolg, M.; Kuechle, W.; Stoll, H.; Preuss, H. *Mol. Phys.* **1993**, *80*, 1431. Kuechle, W.; Dolg, M.; Stoll, H.; Preuss, H. *Mol. Phys.* **1991**, *74*, 1245.
- Bishop, D. M. *Adv. Chem. Phys.* **1998**, *104*, 1.
- Bishop, D. M.; Luis, J. M.; Kirtman, B. *J. Chem. Phys.* **1998**, *108*, 10013.
- Amos, R. D.; Alberts, I. L.; Andrews, J. S.; Colwell, S. M.; Handy, N. C.; Jayatilaka, D.; Knowles, P. J.; Kobayashi, R.; Laming, G. L.; Lee, A. M.; Maslen, P. E.; Murray, C. W.; Palmieri, P.; Rice, J. E.; Simandiras, E. M.; Stone, A. J.; Su, M. D.; Tozer, D. J. *CADPAC5.0, The Cambridge Analytic Derivatives Package*; University of Cambridge: Cambridge, UK, 1992.
- Ingamells, V. E.; Papadopoulos, M. G.; Raptis, S. G. *Chem. Phys. Lett.* **1999**, *233*, 484.
- Reis, H.; Papadopoulos, M. G.; Avramopoulos, A. *J. Phys. Chem. A* **2003**, *107*, 3907.
- Torrent-Sucarrat, M.; Solà, M.; Duran, M.; Luis, J. M. *J. Chem. Phys.* **2002**, *116*, 5363. Torrent-Sucarrat, M.; Solà, M.; Duran, M.; Luis, J. M. *J. Chem. Phys.* **2004**, *120*, 6346.
- Frisch, M. J.; Trucks, G. W.; Schlegel, H. B.; Scuseria, G. E.; Robb, M. A.; Cheeseman, V. G.; Montgomery, J. A.; Vreven, T., Jr.; Kudin, K. N.; Burant, J. C.; Millam, J. M.; Iyengar, S. S.; Tomasi, J.; Barone, V.; Mennucci, B.; Cossi, M.; Scalmani, G.; Rega, N.; Petersson, G. A.; Nakatsuji, H.; Hada, M.; Ehara, M.; Toyota, K.; Fukuda, R.; Hasegawa, J.; Ishida, M.; Nakajima, T.; Honda, Y.; Kitao, O.; Nakai, H.; Klene, M.; Li, X.; Knox, J. E.; Hratchian, H. P.; Cross, J. B.; Adamo, C.; Jaramillo, J.; Gomperts, R.; Stratmann, R. E.; Yazyev, O.; Austin, A. J.; Cammi, R.; Pomelli, C.; Ochterski, J. W.; Ayala, P. Y.; Morokuma, K.; Voth, G. A.; Salvador, P.; Dannenberg, J. J.; Zakrzewski, V. G.; Dapprich, S.; Daniels, A. D.; Strain, M. C.; Farkas, O.; Malick, D. K.; Rabuck, A. D.; Raghavachari, K.; Foresman, J. B.; Ortiz, J. V.; Cui, Q.; Baboul, A. G.; Clifford, S.; Cioslowski, J.; Stefanov, B. B.; Liu, G.; Liashenko, A.; Piskorz, P.; Komaromi, I.; Martin, R. L.; Fox, D. J.; Keith, T.; Al-Laham, M. A.;

- Peng, C. Y.; Nanayakkara, A.; Challacombe, M.; Gill, P. M. W.; Johnson, B.; Chen, W.; Wong, M. W.; Gonzalez, C.; Pople, J. A. *Gaussian 03*, revision A.1; Gaussian, Inc.: Pittsburgh, PA, 2003.
- (42) Schmidt, M. W.; Baldridge, K. K.; Boatz, J. A.; Elbert, S. T.; Gordon, M. S.; Jensen, J. H.; Koseki, S.; Matsunaga, N.; Nguyen, K. A.; Su, S. J.; Windus, T. L.; Dupuis, M.; Montgomery, J. A. *J. Comput. Chem.* **1993**, *14*, 1347.
- (43) Amos, R. D.; Alberts, I. L.; Andrews, J. S.; Colwell, S. M.; Handy, N. C.; Jayatilaka, D.; Knowles, P. J.; Kobayashi, R.; Laming, G. L.; Lee, A. M.; Maslen, P. E.; Murray, C. W.; Palmieri, P.; Rice, J. E.; Simandiras, E. M.; Stone, A. J.; Su, M. D.; Tozer, D. J. *CADPAC6.0, The Cambridge Analytic Derivatives Package*; University of Cambridge: Cambridge, UK, 1995.
- (44) Willetts, A.; Gaw, J. F.; Green, W. H.; Handy, N. C. *SPECTRO: A Theoretical Spectroscopy Package*, version 3.0; Cambridge University: Cambridge, UK, 1994.
- (45) Nygaard, L.; Nielsen, J. T.; Kirchner, J.; Maltesen, G.; Rastrup-Andersen, J.; Sorensen, G. O. *J. Mol. Struct.* **1969**, *3*, 491.
- (46) Keglevich, G.; Bocskai, Z.; Keseru, G.; Ujszaszi, K.; Quin, L. D. *J. Am. Chem. Soc.* **1997**, *119*, 5095.
- (47) Cioslowski, J. *J. Am. Chem. Soc.* **1989**, *111*, 8333 and references therein.
- (48) Allen, L. C. *J. Am. Chem. Soc.* **1989**, *111*, 9003.
- (49) Alparone, A.; Millefiori, A.; Millefiori, S. *J. Mol. Struct. (THEOCHEM)* **2003**, *640*, 123.
- (50) Bishop, D. M. *Adv. Quantum Chem.* **1995**, *25*, 1.
- (51) Spackman, M. A. *J. Chem. Phys.* **1991**, *94*, 1288.
- (52) Langhoff, P. W.; Karplus, M. *J. Chem. Phys.* **1970**, *52*, 1435.
- (53) Millefiori, S.; Alparone, A. *Phys. Chem. Chem. Phys.* **2000**, *2*, 2495.
- (54) Alparone, A.; Millefiori, A.; Millefiori, S. *Chem. Phys.* **2004**, *298*, 75.
- (55) Millefiori, S.; Alparone, A. *J. Mol. Struct. (THEOCHEM)* **1998**, *431*, 59.
- (56) Parr, R. G.; Pearson, R. G. *J. Am. Chem. Soc.* **1983**, *105*, 7512.
- (57) Stevens, W.; Basch, H.; Krauss, J. *J. Chem. Phys.* **1984**, *81*, 6023.
- (58) Wilett, G. D.; Baer, T. *J. Am. Chem. Soc.* **1980**, *102*, 6774.
- (59) Modelli, A.; Burrow, P. D. *J. Phys. Chem. A* **2004**, *108*, 5721.
- (60) Meyers, F.; Marder, S. R.; Pierce, B. M.; Brédas, J.-L. *J. Am. Chem. Soc.* **1994**, *116*, 10703. Albert, I. D. L.; Marks, T. J.; Ratner, M. A. *J. Phys. Chem.* **1996**, *100*, 9714. Adant, C.; Brédas, J.-L.; Dupuis, M. *J. Phys. Chem. A* **1997**, *101*, 3025. Champagne, B.; Mosley, D. H.; André, J.-M. *Int. J. Quantum Chem., Quantum Chem. Symp.* **1993**, *27*, 667.
- (61) Chattaraj, P. K.; Sengupta, S. *J. Phys. Chem.* **1996**, *100*, 16126.
- (62) Millefiori, S.; Alparone, A.; Millefiori, A. *J. Chem. Res., Synop.* **1999**, 238.
- (63) Chesnut, D. B.; Davis, K. M. *J. Comput. Chem.* **1996**, *18*, 584; Cyranski, M. K.; Schleyer, P. v. R.; Krygowski, T. M.; Jiao, H.; Hohlneicher, G. *Tetrahedron* **2003**, *59*, 1657. Cyranski, M. K.; Krygowski, T. M.; Katritzky, A. R.; Schleyer, P. v. R. *J. Org. Chem.* **2002**, *67*, 1333.
- (64) Bishop, D. M.; De Kee, D. W. *J. Chem. Phys.* **1996**, *104*, 9876 and references therein.
- (65) Varsanyi, G.; Nyulaszi, L.; Veszpremi, T.; Narisawa, T. *J. Chem. Soc., Perkin Trans. 2* **1982**, 761.
- (66) Millefiori, S.; Alparone, A. *Chem. Phys. Lett.* **2000**, *332*, 175.
- (67) Kamada, K.; Ueda, M.; Nagao, H.; Tawa, K.; Sugino, T.; Shimizu, Y.; Ohta, K. *J. Phys. Chem. A* **2000**, *104*, 4723 and references therein.
- (68) Stiehler, J.; Hinze, J. *J. Phys. B* **1995**, *28*, 4055.
- (69) Torrent-Sucarrat, M.; Luis, J. M.; Kirtman, B. *J. Chem. Phys.* **2005**, *122*, 204108.